

First Results From Herschel-SPIRE Performance Tests

Tanya Lim ^a, Bruce Swinyard ^a, Asier Aramburu ^a, James Bock ^b, Marc Ferlet ^a, Douglas Griffin ^a, Matthew Griffin ^c, Peter Hargrave ^c, Kenneth King ^a, Sarah Leeks ^d, David Naylor ^e, Samuel Ronayette ^{a,e}, Eric Sawyer ^a, Bernhard Schulz ^f, Sunil Sidher ^a, Locke Spencer ^e,
David Smith ^a, Adam Woodcraft ^c

^a Rutherford Appleton Laboratory, CCLRC, Chilton, Didcot, Oxon, OX11 0QX, UK

^b Jet Propulsion Laboratory, 4800 Oak Grove Drive, Pasadena, CA 91109, USA

^c University of Wales, Cardiff, PO Box 913, Cardiff CF24 3YB

^d Astrophysics Missions Division of ESA, ESTEC, Keplerlaan 1, 2200 AG Noordwijk, NL

^e University of Lethbridge, Department of Physics, Lethbridge, Alberta T1K 3M4, Canada

^f Infrared Processing and Analysis Center, California Institute of Technology, Pasadena, CA 91125, USA

ABSTRACT

The Spectral and Photometric Imaging REceiver (SPIRE) is one of the three scientific instruments on the European Space Agency's Herschel mission. At the start of 2004 the Cryogenic Qualification Model (CQM) of SPIRE was tested with the aim of verifying the instrument system design and evaluating key performance parameters. We present a description of the test facility, an overview of the instrument tests carried out on the CQM, and the first results from the analysis of the test data. Instrument optical efficiency and detector noise levels are close to the values expected from unit-level tests, and the SPIRE instrument system works well, with no degradation in performance from stray light, electromagnetic interference or microphonically induced noise. Some anomalies and imperfections in the instrument performance, test set-up, and test procedures have been identified and will be addressed in the next test campaign.

Keywords: Herschel, Far Infrared, Submillimetre, Bolometer, Instrumentation

1. THE SPIRE CRYOGENIC QUALIFICATION MODEL

The Spectral and Photometric Imaging Receiver (SPIRE¹) is one of three instruments to fly on the European Space Agency's Herschel Space Observatory²; SPIRE is designed for direct detection observations in the hitherto little observed 200-700 μm band. It consists of a cold focal plane unit (FPU), which will be located in the Herschel cryostat, and a set of warm electronics units located some distance away on the Herschel service module. When completed, the FPU will comprise a three-band imaging photometer with bands centred at approximately 250, 360 and 520 μm , and an imaging Fourier Transform Spectrometer (FTS) covering 200-670 μm . The detectors for both sub-instruments are feedhorn-coupled NTD spider-web bolometers³ cooled to 300 mK by a closed cycle ³He refrigerator. The refrigerator has a recycle cycle time of less than two hours and a predicted hold time of more than 46 hours. The bolometer signals are conditioned using JFET pre-amplifiers operating at ~ 120 K, situated close to the FPU and connected to the readout electronics via a 7-m long harness. There is no signal multiplexing at the cold end of the system - each bolometer is read out differentially using sinusoidal bias and individual lock-in amplifiers to ensure that the signals do not suffer from excess system noise.

The photometer and spectrometer fields of view are spatially separated and the two sub-instruments do not operate simultaneously. The photometer has a rectangular field of view of 4 x 8 arcmin. (the largest that can be accommodated) and the spectrometer a circular field of view of 2.6 arcmin. The photometer field of view is observed simultaneously in the three spectral bands using two cascaded dichroic beamsplitters, with angular resolution determined in all three bands

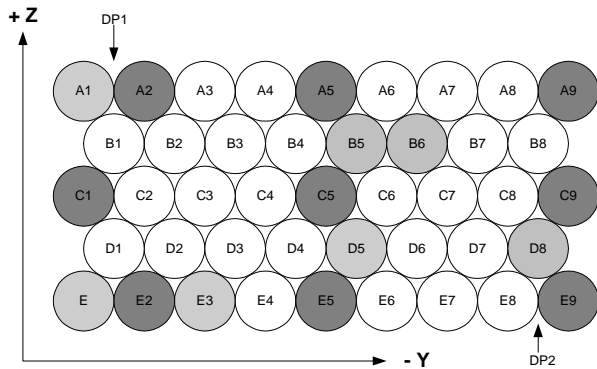


Figure 1: Diagram showing the layout of the photometer CQM engineering grade long wavelength array of 43 detectors. The pixels shaded dark grey are those selected for optical testing. The pixels shaded light grey were non operational.

electronic systems to be operated in as close to flight conditions as possible so that any major problems in the design can be identified ahead of the flight instrument, and to allow a representative cryogenic vibration test to be done on a working instrument, again to allow any major design flaws to be identified before committing to the flight instrument. For cost and schedule reasons, the FPU is not fully equipped with all of the subsystems. It consists of a single channel of the photometer (the longest wavelength band) with an engineering-grade bolometer array (see Figure 1) cooled by a fully representative ^3He refrigerator. The array has several non-functioning pixels and the optical efficiency of the operational pixels is generally lower than the flight specification and exhibits a large spread. Nevertheless, having been thoroughly characterised at unit level, it is adequate for the purpose of evaluating the performance of the rest of the system. Arrays built subsequently for the flight instrument have been tested and meet the performance specifications with good uniformity.

The bolometer signals are conditioned by a single 48-channel JFET amplifier module; seven other JFET modules are replaced by dummy resistor networks the provide a passive but representative load to the warm lock-in amplifiers. The full set of instrument optics, filters, and dichroics is fitted as the pass-band is controlled by the combination of all the filters within the SPIRE instrument. The beam steering mirror is replaced by a mass thermal dummy as are the other four detector arrays and the spectrometer scan mechanism. Both the photometer and spectrometer calibrators are engineering grade units with the correct mass and thermal characteristics and near-flight-level performance. The analogue and digital electronics used to drive the instrument are engineering quality with flight functionally, and a working version of the instrument on-board software has been installed to produce representative telemetry streams.

In this paper we discuss the tests carried out during the initial performance testing of the CQM, and present some of the results of those tests. First we describe the test facility used and give an outline of the test programme and the rationale behind this first operation of the entire SPIRE system.

2. THE SPIRE INSTRUMENT TEST FACILITY

The cryogenic test facility⁴ has two working areas: a clean room housing the custom-built SPIRE test cryostat and optical benches, and a control room housing the instrument Electronic Ground Support Equipment (EGSE) and Test Facility Control Equipment (TFCS). The clean room is at class 10,000 except in the area of the cryostat where the class is 1000. The cryostat simulates the thermal conditions provided by the Herschel cryostat with temperature stages of 7-11 K, 4.2 K and 1.7 K. The instrument can view a room-temperature telescope simulator via a PTFE window on the cryostat vacuum vessel. A set of thermal filters on the liquid nitrogen cooled cryostat shield and the helium gas-cooled “10-K” shield remove most of the thermal infrared from the ambient room background. A pair of neutral density filters

by the telescope diffraction limit. The FWHM beam widths will be approximately 17, 24 and 35" at 250, 360 and 520 μm respectively. An internal beam steering mirror allows spatial modulation of the telescope beam for both photometer and spectrometer. Mapping observations can also be made by scanning the telescope. The spectrometer uses a dual-beam (Mach-Zehnder) configuration with broad-band intensity beam dividers. The FTS scanning mirror has a linear travel of up to 3.5 cm, providing adjustable spectral resolution from 0.04 - 2 cm^{-1} ($\lambda/\Delta\lambda = 20 - 1000$ at 250 μm).

The SPIRE cryogenic qualification model (CQM) is the first instrument model built to undergo performance testing. The cold focal plane unit comprises a combination of flight like components and mass dummies. It has been built to serve two main purposes: to allow the optical, thermal, and

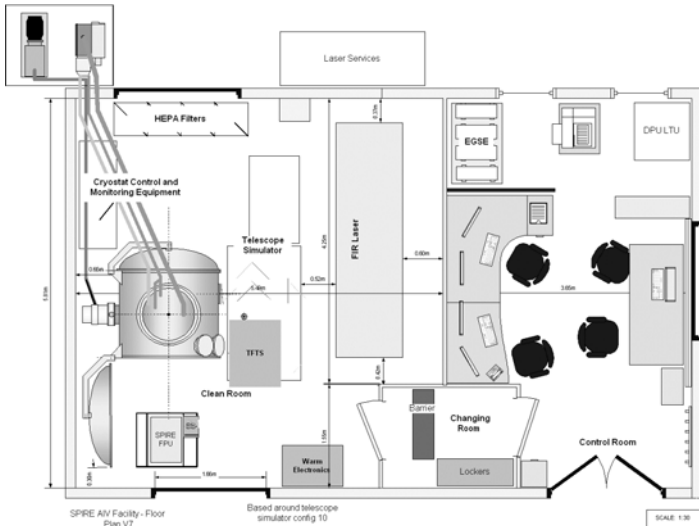


Figure 2: The SPIRE test facility plan.

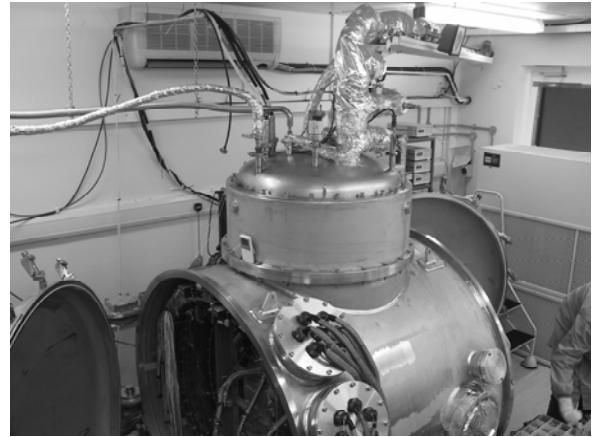


Figure 3: Photograph of the SPIRE test cryostat

placed on the 4.2-K shield reduces the in-band radiant background to a level equivalent to that expected from the 80-K, 4% emissive Herschel telescope. A cryogenic black body source is also provided inside the cryostat. This can be viewed directly by the instrument via a flip mirror, and completely fills the instrument field of view. When the cryogenic black body is unheated it is used as the dark reference for the instrument, and when it is heated it can reach up to 40 K in a few tens of minutes. The performance of the cryostat was nominal with hold times, when completely filled, of more than 24 hours.

Two external sources, a hot black body and a far infrared laser, can be coupled to SPIRE via a 300-K telescope simulator situated on a low level optical bench next to the cryostat. The telescope simulator presents the instrument with an $f/8.68$ beam via a pupil mask which correctly represents the input from the Herschel telescope. Two fold mirrors within the simulator optical train can be scanned to place a source at the input of the telescope simulator anywhere within the SPIRE field of view.

The adjustable-temperature black body source is used as the input source to a test FTS⁵ (TFTS), the output of which is coupled to the input of the telescope simulator. The TFTS provides a spectral scan of the black body allowing measurement of the photometer spectral response. With the FTS mirrors stationary, the same black body provides a point source which can be scanned over the SPIRE field of view. The telescope simulator and TFTS are situated in a dry air enclosure allowing operation in relative humidity as low as 6-10%. The optical configuration can be manually changed to place the blackbody in the telescope simulator pupil plane and the two scanning mirrors can then be used to scan the point source laterally to measure the illumination pattern with which the SPIRE detector feedhorns will illuminate the secondary mirror of the Herschel telescope.

The far infrared laser is an Edinburgh Instruments model PL295 gas laser, pumped by a CO₂ laser equipped with an active stabilisation system to ensure constant laser power output. The laser gives a range of lines from 10.6 μm to 2 mm and there are numerous lines covering the SPIRE band. For the CQM test campaign the 432.631/432.666 μm doublet line from formic acid was selected as it had good stability, is not attenuated by the atmosphere and gave a maximum output power between 5 - 10 mW.

3. OVERVIEW OF THE TEST PROGRAMME

The performance tests were divided into three basic types: thermal balance, during which the basic thermal design of the instrument was evaluated, 'closed' cryostat testing with the instrument viewing the internal cryogenic black body, and optical testing with the instrument viewing the telescope simulator via the cryostat entrance window.

Thermal balance tests: The most basic of these was to ensure that the different temperature stages of both the cryostat and the instrument achieved the required temperatures. All temperatures were as expected during testing with the exception of the 1.7-K stage which ran colder than expected (1.4 K) due to an inability to control the pressure above the helium in the cryostat He-II tank – this will be rectified for the next test campaign. Once the cryostat temperature stages were verified, the ^3He cooler was recycled by command through the instrument electronics. Within two hours of the start of the cooler cycle operation, the cold tip achieved a temperature of < 270 mK and the cooler subsequently held for over 60 hrs, albeit with a much reduced load compared to that expected in flight as only one detector array was connected and the 1.7-K stage was operating at a reduced temperature.

Closed cryostat tests: One of the most important objectives of the SPIRE CQM test programme was to prove that the integrated system (FPU + harness + warm electronics) will function correctly and that no excess noise is introduced due to ground loops, electromagnetic interference, bias supply noise, microphonics, etc. To this end noise measurements were carried out both on the resistor networks in the dummy JFET units and on the detectors when biased under minimum photon background conditions. We were also able to measure the V-I characteristics (hereinafter “load curves”) of the detectors under a number of different bias and optical load conditions, using the cryogenic black body to increase the photon background. In this way we could measure directly the temperature increases in the bolometers and relate these to the absorbed power levels. The results of the noise and load curve measurements are reported in the Section 4.

Optical tests: The external source and the telescope simulator were used to measure the centre positions of several pixels and to measure in detail the beam profile on the sky of the central detector. The TFTS was used to measure the spectral band of the same set of pixels. The external source was also used to illuminate the pupil to measure the conjugate beam response of a single pixel (this test was only partially successful as discussed below). Finally, the laser was used to illuminate the array to search for stray light glints and to verify the frequency response of the detectors using a variable frequency chopper. We report on the optical test results in Section 5.

4. CLOSED CRYOSTAT TESTING

4.1. Noise

The noise was measured through the complete system in three different ways:

- (i) with the bolometers at a temperature of > 1.7 K, and therefore of very low impedance - this measured the input-short noise of the complete electronics chain (JFETs, cryo-harness, and warm electronics) in isolation;
- (ii) using the resistor network in the dummy JFET units - this measured the noise with the bias circuit operating but without the presence of thermal noise from the detectors;
- (iii) with the detectors under nominal bias, temperature, and photon background - this measured the complete system noise in a fully representative situation.

With these three tests we were able to check for extraneous system noise compared to that predicted from the measurements of the individual components and, if any were seen, we could isolate the part of the system where the noise arose. We saw no excess noise over and above that expected from previous unit-level tests on the component parts. By making a change in the grounding within the cryo-harness, we also showed that the grounding and shielding scheme employed is optimum for the protection of the SPIRE instrument from external sources of EMI. Figure 4 shows examples of the noise spectra taken with detectors under nominal bias conditions: the spectra show no $1/f$ type noise down to 10 mHz – better than the goal of 30 mHz. The excess noise peak at very low frequencies is due to the drift in the temperature stages in the cryostat which take many hours to stabilise following cryogen filling operations.

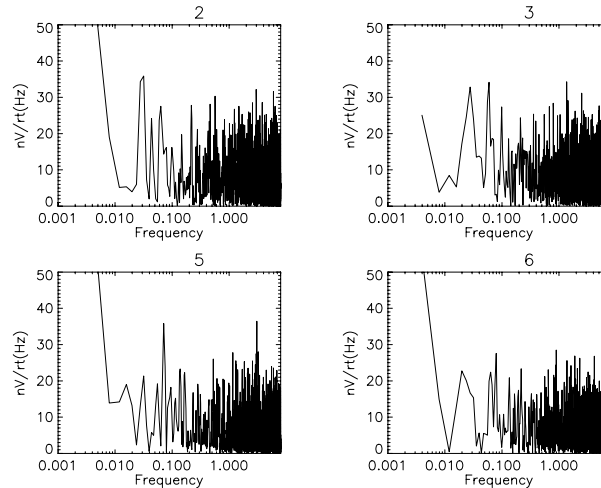


Figure 4: Measured noise spectra of four CQM detectors. The spectrum of the electrical noise is flat over the expected operating band of the SPIRE photometer (0.03-5 Hz). The excess noise below 10 mHz is due to thermal drifts in the cryogenic test facility.

4.2. Load Curves

Load curves (measurements of the bolometer voltage as a function of current) enable parameters describing the electrical and thermal properties of a doped germanium bolometer to be determined^{7,8}. The performance of the bolometer can then be predicted for different operating conditions. Load curves can also be used to calculate the radiant power absorbed by a bolometer.

Load curves are most naturally measured using a DC bias. However, for these tests the flight electronics were used which, for noise performance reasons, use an AC bias. In order to determine that we were correctly compensating for frequency dependent effects, load curves were measured using several bias frequencies, and the in and out of phase detector voltage was measured. The load curves measured at different frequencies were in good agreement once they had been corrected for frequency dependent effects. DC load curves had previously been measured for this array at unit-level (at JPL before it was shipped for integration with the instrument). Some discrepancies remain between the AC and DC load curves: these are currently being investigated.

Figure 5 shows load example curves measured on one of the CQM bolometers when viewing different black body temperatures. The effect of loading from the black body can clearly be seen as a suppression of the measured voltage. Results for other bolometers were similar. The solid lines show the results of fitting an ideal bolometer model⁷ to the measured data: good fits were obtained for all operating bolometers in the array, demonstrating that all the bolometers are well-characterised by the bolometer model. The model requires accurate knowledge of the bolometer resistance as a function of temperature; the range of temperatures available in these tests did not permit this to be determined, and values measured in unit-level testing of the array at JPL were therefore used. The derived values of parameters describing the thermal conductance between the bolometer absorber and heat sink were in good agreement with the values measured at JPL.

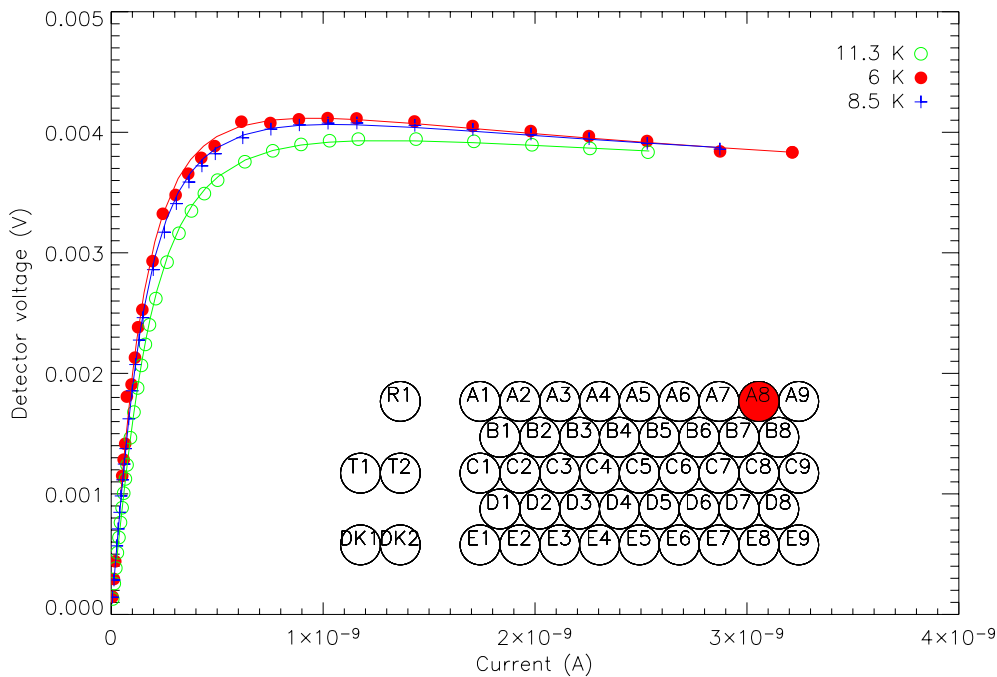


Figure 5: Load curves for detector A8. The filled circles are the dark case, the open circles are for the black body at 8.5 K case and the crosses are for the black body at 11 K.

4.3. Detector Optical efficiency

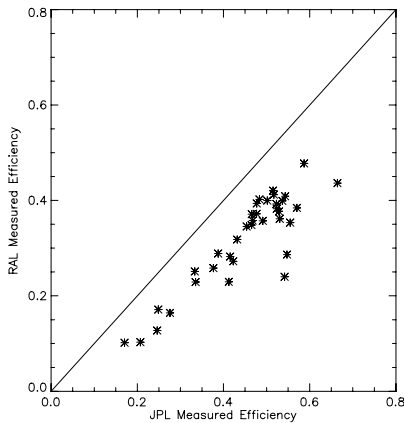


Figure 6: Comparison of estimated detector optical efficiency measured at JPL and RAL. The stars represent individual pixels within the CQM array. The large spread in optical efficiency for different pixels is because this was a non-science grade array. This pattern is not repeated in the flight units.

The overall optical efficiency of the instrument can be measured by comparing the temperature rise seen with the cold blackbody at two different temperatures and calculating the absorbed power using the detector parameters measured on the array at unit level. Data were obtained for temperatures of 8.5 K and 11 K. By subtracting the 8.5-K measured power from the 11-K measured power and dividing by the expected power using knowledge of the instrument passband from the measurement of the individual filters and making some assumptions about the instrument throughput and black body emissivity, we can calculate the optical efficiency of the detectors and compare it to that measured during array testing at JPL. Figure 6 shows the comparison between the RAL and the JPL measurements. The general trend is reproduced between the two measurements to within 20% (the RAL figures being systematically lower than the JPL figures). This difference could be due to a number of factors in the calculations from the data from either measurement. There is clearly more work to be done to understand the difference, but the results have demonstrated that the overall efficiency of the optics and filters is within specification.

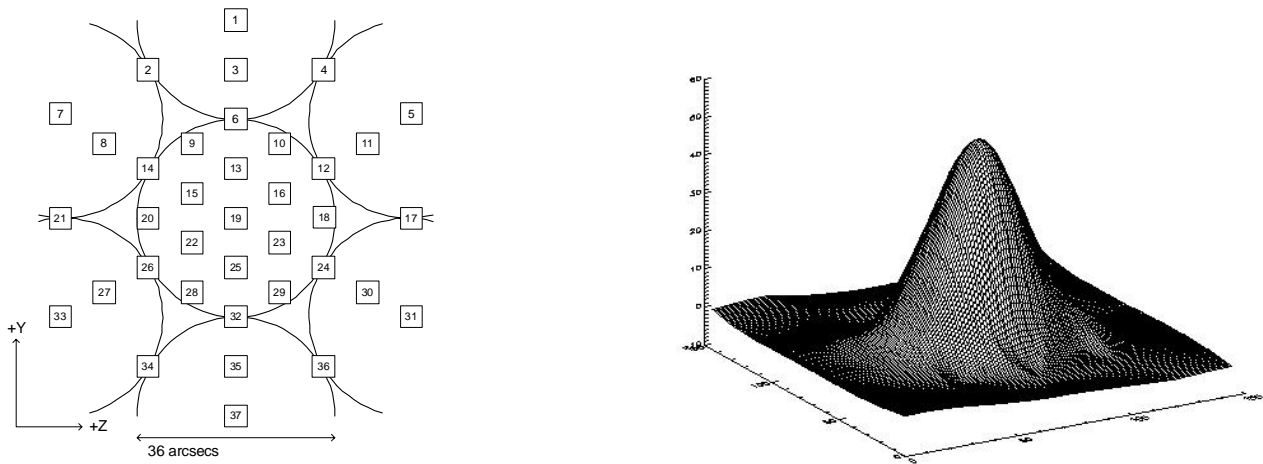


Figure 7: The scan pattern used for the beam profile measurement (left) and the resulting beam re-gridded onto a square grid (right).

5. OPTICAL TESTING

5.1. Sky beam profile tests

The simulated beam profile on the sky was only measured on the central pixel C5. This was done by fine scanning the hot black body across the beam via the telescope simulator as shown in Figure 7. A manual variable iris aperture is set to a diameter much smaller than the diffraction spot at the entrance focal plane of telescope simulator (providing 1:1 imaging) in order to simulate a point source as observed by SPIRE. The average FWHM was found to be $37.4 \pm 1.9''$, somewhat broader than the expected value of $34''$ from analysis of the feedhorn beam profile and the diffraction pattern produced by the telescope simulator. The most likely explanation for the slight broadening is some pupil and field misalignment at the interface between SPIRE (inside the cryostat) and the telescope simulator (outside the cryostat) and between the source and the telescope simulator. This will be investigated in the next test campaign.

5.2. Pupil illumination tests

To map the beam profile with which the detectors illuminate the telescope pupil, the hot blackbody source was imaged at a SPIRE pupil plane and moved in one axis. Figure 8 shows the signal on a particular detector plotted as a function of the position of the source in the pupil. The main feature to notice is the dip in the signal in the middle of the curve due to the hole in the beam steering mirror for the calibration source. This hole fits the central obstruction in Herschel's pupil due to the secondary mirror.

The scan was performed the same way as the scan of the focal plane, i.e. using the flat mirrors of the telescope simulator. The actuator ranges do not allow us to fully scan the pupil and it was only possible to perform a scan along about $\sim 75\%$ of a diameter of the pupil without resetting the optical system; in this test run we did not have time to complete this test but rather just to prove the concept of the measurement. There were also problems with vignetting of the pupil image due an error in setting up the telescope simulator. In order to fully understand the data we plan repeating the measurements in the next tests using the laser source to give a higher signal to noise.

5.3. Ghosts and glints

The array was checked for ghosting using the external black body source to look for response in the un-illuminated detectors. Early results show no indications of ghosting above a few percent. When illuminated with a high power level from the far infrared laser, one edge of the array was seen to be illuminated preferentially. This may be due to a glint from the SPIRE structure close to the entrance focal plane. The CQM was built without the full stray light control measures and we expect this issue to be solved for the flight model by the incorporation of absorbing material around the focal plane baffle.

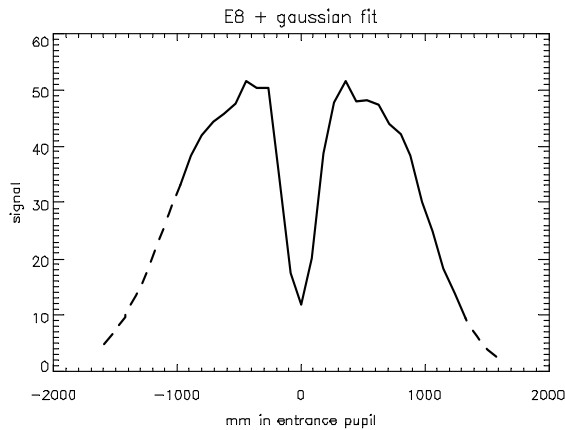


Figure 8: Pupil scan measurement results for a single pixel given as detector response in arbitrary units versus pupil distance at the Herschel primary mirror (in mm). The dotted lines show a modelled continuation of the response assuming a Gaussian response function for the detectors.

6. CONCLUSIONS AND PLANS FOR FUTURE TEST CAMPAIGNS

While various problems and anomalies arose in this first operation of a complex instrument, the CQM test campaign has successfully demonstrated that the complete system (thermal, electrical, optical, software, EGSE) functions well. No major problems arose with stray light, EMI, excess noise or microphonic disturbances. The bolometer noise levels were measured through the complete instrument chain and were found to be in good agreement with the results expected from unit-level tests on the detector array. The instrument optical efficiency as estimated from bolometer load curve data is within specification and in good agreement with that predicted from unit-level measurements on the individual components. The FPU has been subjected to cryogenic vibration testing and has survived

Various improvements in the test equipment and methods are planned for the next CQM cold test, and for future testing of the SPIRE flight instrument. In particular:

- (i) an independent baseline measurement of the test facility optics efficiency, spectral response will be made using a separate ^4He bolometer system in the position of the SPIRE FPU;
- (ii) the load curve measurement system will be adapted to allow DC load curves to be obtained, and measurements will be made over a wider range of cryogenic black body temperatures to permit a more accurate estimation of the photon background and instrument efficiency;
- (iii) an improved air-drying system will be implemented for FTS spectral measurements;
- (iv) beam profiles will be measured over the whole array;
- (v) the instrument 300-mK and 1.7-K thermal architecture will be made more representative to allow the ^3He cooler performance to be evaluated in more flight-like conditions.

The CQM was first tested in February 2004, after which it was subjected to cold vibration testing at CSL, Liege. At the time of writing it is being prepared for post-vibration functional and performance tests at RAL. Following these tests it

will be delivered to the Herschel industrial contractor for system-level testing together with the other Herschel instrument CQMs.

Testing of the SPIRE flight instrument is planned to take place between Autumn 2004 and Summer 2005, with delivery in late 2005.

REFERENCES

1. M. Griffin, B. Swinyard, and L. Vigroux, *The Herschel-SPIRE instrument*, Proc. SPIE 5487 (this volume), Glasgow, 21-25 June 2004.
2. G. Pilbratt, *Herschel Mission: status and observing opportunities*, Proc. SPIE 5487 (this volume), Glasgow, 21-25 June 2004.
3. B. Rownd, J.J. Bock, G. Chattopadhyay, J. Glenn and M. Griffin, *Design and performance of feedhorn-coupled arrays coupled to submillimeter bolometers for the SPIRE instrument aboard the Herschel Space Observatory*, Proc. SPIE 4855, 510-519, 2003.
4. P.A. Collins, D.L. Smith, M. Ferlet, T. Grundy, M. Harman, M. J. Griffin, P.A.R. Ade, and B. M. Swinyard, *Ground calibration facility for Herschel-SPIRE*, Proc. SPIE 4850, 628-637, 2003.
5. L. Spencer, D. Naylor, B. Swinyard, A. Abreu Aramburu, T. Fulton, T. Lim, S. Ronayette, and I. Schofield, *A Fourier transform spectrometer for ground testing of the Herschel/SPIRE instrument*, Proc. SPIE 5487 (this volume), Glasgow, 21-25 June 2004.
6. K. Dohlen, A. Origne, and M. Ferlet, *Optical alignment verification of the Herschel-SPIRE instrument*, Proc. SPIE 5487 (this volume), Glasgow, 21-25 June 2004.
7. R.V. Sudiwala, M.J. Griffin, and A.L. Woodcraft, *Thermal Modelling and Characterisation of Semiconductor Bolometers*, Int. Journal of Infrared and Mm Waves, 23, 545, 2002.
8. A.L. Woodcraft, R.V. Sudiwala, M.J. Griffin, E. Wakui, B. Maffei, C.E. Tucker, C.V. Haynes, F. Gannaway, P.A.R. Ade, J.J. Bock, A.D. Turner, S. Sethuraman, J.W. Beeman, *High Precision Characterisation of Semiconductor Bolometers*, Int. Journal of Infrared and Mm Waves, 23, 575, 2002.